Materials Science Forum
ISSN: 1662-9752, Vol. 1062, pp 49-53
doi:10.4028/p-f26rb5

Submitted: 2021-10-14
Revised: 2022-02-22
Accepted: 2022-03-07
Online: 2022-05-31

Impact of Epitaxial Defects on Device Behavior and their Correlation to the Reverse Characteristics of SiC Devices

E. Kodolitsch[1,2a*], V. Sodan[2b], M. Krieger[1c], N. Tsavdaris[2d]

[1]Lehrstuhl für Angewandte Physik, Department Physik, Friedrich-Alexander-Universität Erlangen-Nürnberg, Staudtstraße 7, 91058 Erlangen, Germany

[2]Infineon Technologies Austria AG, Siemensstraße 2, 9500 Villach, Austria

[a]Elisabeth.kodolitsch@infineon.com, [b]Vice.Sodan@infineon.com, [c]Michael.krieger@fau.de, [d]Nikolaos.Tsavdaris@infineon.com

Keywords: 4H-SiC, extended defects; photon emission microscopy, electrical characterization

Abstract. In this work we report on the impact of various crystalline defects present in 4H-SiC epitaxial layers on the electrical blocking characteristics of SiC power devices. Dedicated test structures were fabricated and electrically characterized in reverse bias mode. SiC substrate and epitaxial crystal defects, as well defects due to front-end processing were detected and classified using commercial inspection tools. Devices with a single defect-type were studied which leads to a direct correlation of the leakage current spot position within the device and the obtained blocking characteristics. This gives a better understanding of each crystal defect impact on device´s performance which leads to an improvement in the reliability and cost reduction of SiC power devices.

Introduction

In the recent years, silicon carbide (SiC) technology started showing a continuous raise in market share for high power electronic applications, as the SiC devices display a higher performance, efficiency and reliability. However, despite a rapid development in SiC bulk material, crystal defects are still present in both SiC substrates and epitaxial layers leading to a reduction of the overall yield. In order to ensure a device performance close to the theoretical limits, it is essential to have a better understanding of the impact of such crystal defects on SiC device characteristics. Several studies have already reported the effect of surface and crystalline defects such as carrots, micropipes and triangle epitaxial defects on reverse device characteristics [1-7]. These reports focus either on high volume statistics analysis or specific case studies. However, the presence of multiple type of defects per device, their density and location in both active and passive areas of the devices, as well as the variety of devices and specifications reported, makes it difficult to draw clear conclusions over the kill rate of each crystal defect and their exact role in the failing mechanism.

In this contribution, we focus on analyzing the influence of crystalline defects on the reverse characteristics that can lead to a reduced blocking capability of SiC power devices. Hence, for the study devices that contain only one type of crystal defect per device were considered. Photon emission microscopy (PEM) observations combined with the recorded reverse characteristics, allow a direct correlation between the screened epitaxial defects and the tested devices.

Experimental

N-type epitaxial layers were grown on 4° off-axis towards [11-20] direction 4H-SiC substrates. Epitaxial defects were localized and classified algorithmically on a commercially available inspection tool, using an optical microscope along with a photoluminescence (PL) channel that is operating with a 660 nm long pass filter. Dedicated SiC test structures containing an active area (p-n junction) and an edge termination were fabricated and related voltage blocking characteristics were studied. Devices with a single defect type were selected and clustered into two distinctive groups: devices which show intrinsic behavior and devices which show increased leakage currents (exceeding the μA

range at total electric field over the epi layer up to $1.4x10^6$ V/cm). This classification enables the study of both scenarios for devices containing the same defect type. Backside PEM analysis was performed in order to localize the exact position of leakage current spots within the devices. PEM is used to detect photonic radiation from a defective site within the devices due to excessive heat generation. The emission is thereby detected with highly sensitive cameras and gives information on potential failure positions.

Results and Discussion

To analyze and understand the behavior of each defect type on the blocking characteristics, we looked towards devices with a specific one-type defect per device. Fig. 1 shows the optical microscopy and photoluminescence images of the six most common killer defects under investigation: 1 (a-b) triangular defects with a 3C-SiC inclusion , 2 (a-b) Frank-type defects (includes a stacking fault in the basal plane and also in the prismatic plane) , 3 (a-b) micropipes, 4 (a-b) nano-scale pits, 5 (a-b) Shockley type stacking faults (SSF), and 6 (a-b) carrots type defects.

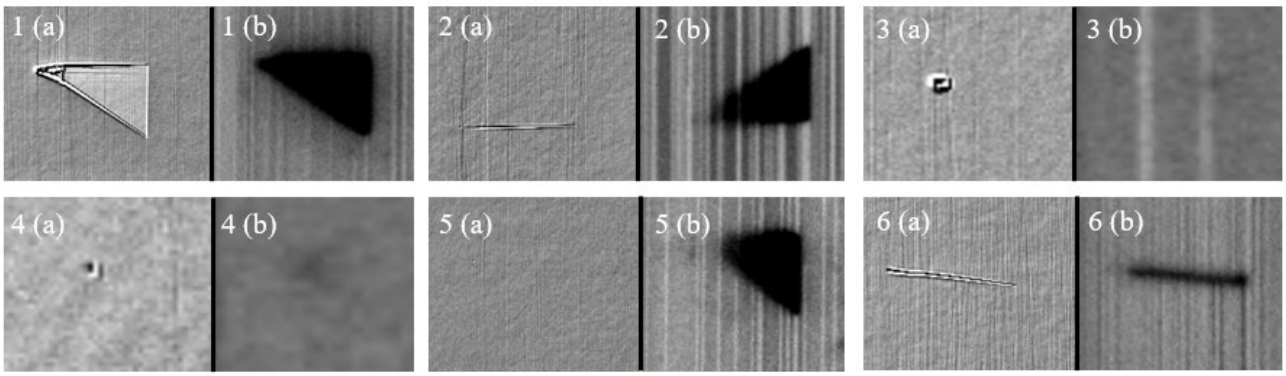

Figure 1. Optical microscopy (a) and photoluminescence images (b) of defect-types: triangular defects (1), Frank-type defect (2), micropipes (3), nano-scale pits (4), stacking faults (5) and carrots (6)

While most of the defects mentioned above showing characteristic surface morphology features, only SSFs do not show any surface feature and are only detectable due to their distinctive PL signal. The reverse characteristics of devices containing only one single defect type were recorded and compared to a reference (defect-free) device showing intrinsic behavior. The measured reverse leakage current as a function of the electrical field is shown in Fig. 2.

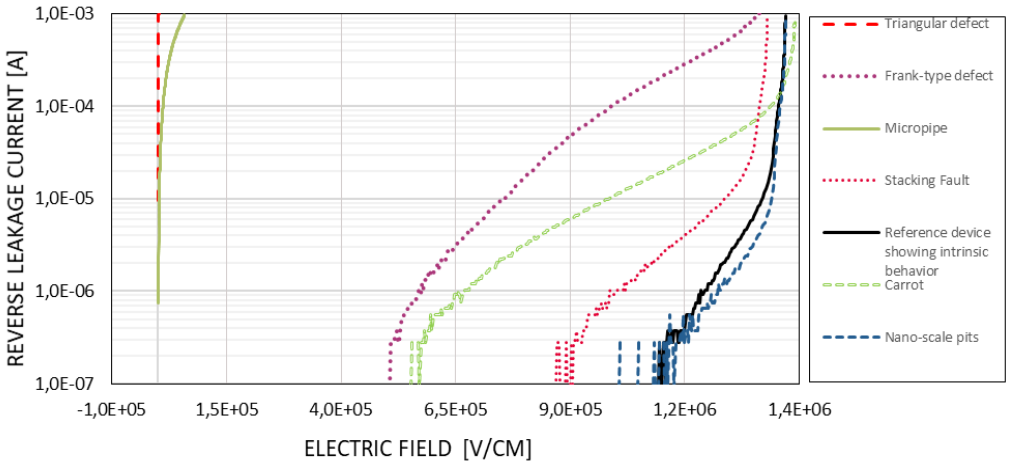

Figure 2. Reverse leakage current characteristics vs. electrical field of SiC devices with one-type defect per device and without as reference (see black curve).

Devices with triangular defects (see Fig.1 (1a-b)) results to one order of magnitude higher leakage current compared to the reference device and show an ohmic behavior by already applying very low voltages (case of only one device is shown in Fig.2). PEM emission spots were detected directly on the triangular defect position for all studied devices (Fig.3). Moreover, the leakage emission spots seem to be independent of the defect position within the device, such as, the active p-n junction area and/or the edge termination region. It has been predicted theoretically that the bandgap at a local polytype change is reduced, thus leading to an increase of the leakage current [8].

Similar blocking characteristics as the one described above were identified on devices with micropipe-type defects originated from the substrate. However, from the PEM analysis, it was found that micropipes only lead to increased leakage current if they are located in the active p-n junction area. In 40% of the tested devices the micropipe defect was located at the edge termination region, which did not result to an increased leakage current. Micropipes were described to act as direct leakage current path through the device, also on earlier studies [9].

On the other hand, devices that contain Frank-type stacking faults (FSFs) and carrots defects showed high device- to- device variations. Accordingly, some devices display no reduction in the blocking capabilities, while other devices showed a significant variation of the leakage currents ranging from few nanoampere (nA) to several microampere (μA). PEM analysis reveals that emission spots were along the defects´ surface feature (Fig. 3 (b-c)). The emission spots on these devices could only be detected when the defect was situated in the active p-n junction area.

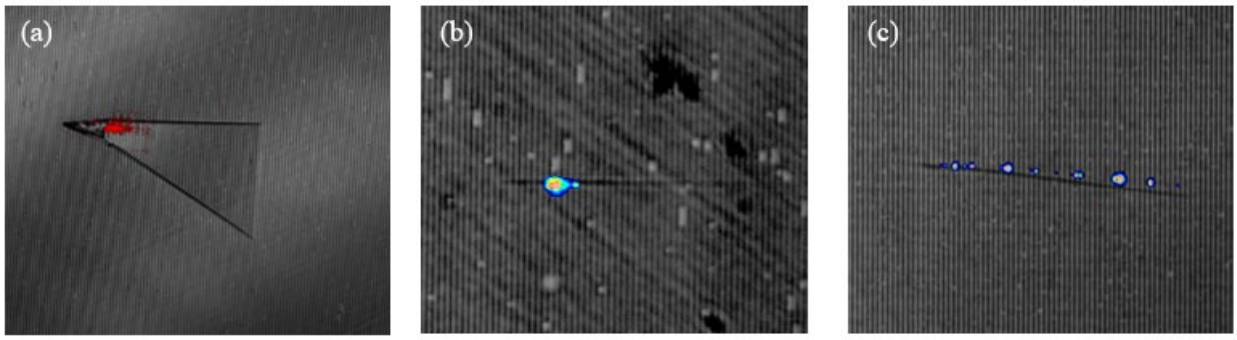

Figure 3. Photon emission microscopy (PEM) spots detected on the devices with a defect-type as: triangular defect (a), a Frank-type defect (b) and a carrot (c).

In order to have a correct overview of the defect contribution (i.e. defect surface or volume impact) to the obtained blocking characteristics, chemical mechanical polishing (CMP) was carried out on the grown layer after epitaxy process.

The surface feature of FSFs and carrot defects can vary both in shape and depth and is known to be the indication of an underlying prismatic stacking fault [10, 11]. The CMP resulted in a smoother surface feature of the defects as displayed in Fig. 4 (Ia and IIa). Subsequently, device processing and testing was implemented and PEM analysis was carried out on one device that shows an increased leakage current and contains a carrot defect (Fig. 4 III). The position of the emission spot is located at the area of the prismatic SF, similar to the devices without the CMP process. Thus, the defect surface feature does not contribute in the reduction of the blocking capability but instead it is the prismatic stacking fault within the epitaxial layer volume (Fig. 4 IV).

Devices containing Shockley type stacking faults (Fig.1 (5a-b)) showed reverse characteristics comparable with the ones obtained on the reference device (see Fig.2). A correlation of the defect position with the emission spots observed by PEM was only found in two out of twelve devices, at electric fields above $1x10^6$ V/cm implicating no negative affect on the blocking characteristics, neither if located in the active p-n junction area of the device nor in the termination region.

While for all above-mentioned defect types per device a correlation, in some cases more pronounced, could be found, no clear correlation was found for single nano-scale pits type defects. These defects are approximately 200 nm in diameter and associated to substrate threading dislocations. It was shown in literature that the topology of these defects type can influence leakage

current and breakdown voltage in SiC p-n and Schottky diodes [12, 13]. Based on the results displayed in Fig. 2, no increase of the reverse characteristics, neither leakage current emission spots on the defect position could be observed.

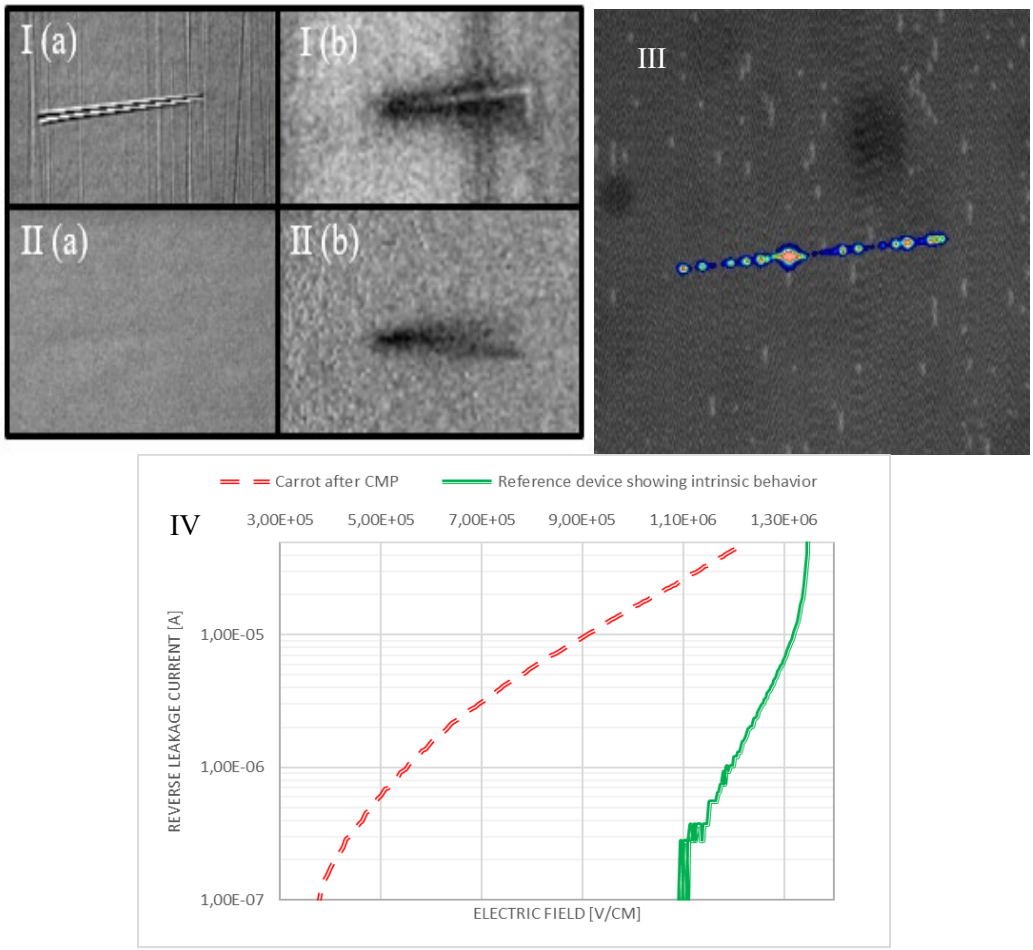

Figure 4. Optical microscope (a) and the PL channel (b) images of devices with carrot-type defects prior (I) and after chemical mechanical polishing CMP (II). PEM spots were observed on the position of the prismatic SF (III) leading to an increased leakage current in comparison to a reference device (defect free) (IV).

Summary

In this work, a direct correlation between various crystal defect types, their location and impact on the reverse leakage current of SiC devices was performed. Devices with a single defect were selected for this study and PEM analysis was carried out, to verify the position of the defect and the leakage current spots. Devices containing a triangular defect with a 3C-SiC inclusion or a micropipe showed leakage current with a clear ohmic behavior at a very low electric field. For devices containing Frank-type SF and carrot defects, we observed high device-to-device variations of the blocking capabilities. Leakage current spots on those devices were located at the position of the prismatic SF of the defect. This is independent of the surface feature of the defects as demonstrated for wafers with CMP treated surface. No significant correlation was found for devices that contain a Shockley type stacking fault or a nano-scale pit. The evaluation of the impact of various defects on the leakage current fails is essential towards the improvement of reliability and cost reduction of SiC power devices.

References

[1] T. Kimoto et al., Prog. Cryst. Growth Charact. Mater. 62, (2016), 329-351

[2] J. Zhao et al., Nanotechnol. Precis. Eng. 3, (2020), 229

[3] R. Konishi et al., Japanese J. Appl. Phys. 52 (2013)

[4] H. Jung et al., Materials Science Forum 821-823, (2015), 563-566

[5] T. Katsuno and Y. Watanabe et al., Japanese J. Appl. Phys. 50 (2011)

[6] E. Van Brunt et al., Materials Science Forum 924, (2018), 137-142

[7] H. Das et al., ECS Transactions 80, (2017), 239-243

[8] U. Lindefelt et al., in Silicon Carbide- Recent Major Advances (eds W. J. Choyke, H. Matsunami and G. Pensl), Springer, (2004), pp.89

[9] P. Neudeck et al., IEEE Electron Device Letter 15, (1994), 63

[10] Zhang et al., Mater. Sci. Forum 527-529, (2006), 327-332

[11] Dong L. et al., Mater. Sci. Forum 778-780, (2014), 354-357

[12] J. Schoeck et al., Materials Science Forum 924, (2018), 164-167

[13] P. G. Neudeck et al., Materials Science Forum 338-342, (2000), 1161-66